

# Macroscopic description of current induced switching due to spin-transfer

J. Barnaś<sup>1,2</sup>, A. Fert<sup>3</sup>, M. Gmitra<sup>1</sup>, I. Weymann<sup>1</sup>, and V. K. Dugaev<sup>4</sup>

<sup>1</sup>*Department of Physics, Adam Mickiewicz University, Umultowska 85, 61-614 Poznań,*

<sup>2</sup>*Institute of Molecular Physics, Polish Academy of Sciences,  
M. Smoluchowskiego 17, 60-179 Poznań, Poland*

<sup>3</sup>*Unité Mixte de Physique CNRS/THALES associated with  
Université Paris-Sud, Domaine de Corbeville, 91404 Orsay, France*

<sup>4</sup>*Department of Physics and CFIF, Instituto Superior Tecnico, Av. Rovisco Pais, 1049-001, Lisbon,  
Portugal; and Institute for Problems of Materials Science, NASU, Vilde 5, 58001 Chernovtsy, Ukraine*

(Dated: November 21, 2018)

We develop a macroscopic description of the current-induced torque due to spin transfer in a layered system consisting of two ferromagnetic layers separated by a nonmagnetic layer. The description is based on i) the classical spin diffusion equations for the distribution functions used in the theory of CPP-GMR, ii) the relevant boundary conditions for the longitudinal and transverse components of the spin current in the situation of quasi-interfacial absorption of the transverse components in a magnetic layer. The torque is expressed as a function of the usual parameters derived from CPP-GMR experiments and two additional parameters involved in the transverse boundary conditions. Our model is used to describe qualitatively normal and inverse switching phenomena studied in recent experiments. We also present a structure for which we predict only states of steady precession above a certain critical current. We finally discuss the limits of a small angle between magnetic moments of the ferromagnetic layers and of vanishing imaginary part of the mixing conductance.

PACS numbers: 75.60.Ch, 75.70.Cn, 75.70.Pa

## I. INTRODUCTION

The magnetic moment of a ferromagnetic body can be switched without applying an external magnetic field, but only by transfer of electron spins carried in a spin polarized current. The concept of spin transfer has been introduced by Slonczewski<sup>1</sup> and appears also in several papers of Berger<sup>2</sup>. Magnetic switching by a spin polarized current has been now confirmed in extensive series of experiments<sup>3,4,5,6</sup>. Spin transfer is also an important turning point in spintronics. In spintronic phenomena of the first generation, like giant magnetoresistance (GMR)<sup>7</sup> or tunneling magnetoresistance (TMR)<sup>8</sup>, the magnetic configuration of a nanostructure is detected by an electrical current. On the contrary, in spin transfer experiments a magnetic configuration is created by a current. This possibility of back and forth magnetic switching opens new fields for spintronics.

Current-induced magnetic switching (CIMS) has been clearly demonstrated<sup>4</sup> by experiments on structures F1/N/F2 consisting of two ferromagnetic layers of different thicknesses separated by a nonmagnetic layer N. Starting from a parallel configuration of the magnetizations in F1 and F2, a current exceeding a certain critical value can reverse the magnetic moment of the thinner magnetic layer to set up an antiparallel configuration. In turn, a current in the opposite direction can switch back the structure to the parallel configuration. With an applied field, the spin transfer mechanism can also generate a steady precession of the magnetization, detected by oscillations of the current in the microwave frequency range<sup>9</sup>.

In the concept introduced by Slonczewski<sup>1</sup>, as well as in most theoretical models<sup>10,11,12</sup>, the current-induced torque acting on the magnetization of a magnetic layer is related to the spin polarization of the current and, more precisely, to the absorption of the transverse component of the spin current by the magnetic layer. From CPP-GMR experiments one knows that the spin polarization of the current is due to spin dependent reflections at interfaces and to spin dependent scattering within the magnetic layers. For CIMS, similarly, recent experiments<sup>6</sup> have shown that the switching currents can be modified and even reversed by doping the magnetic layers with impurities of selected spin dependent scattering cross-sections.

Both CPP-GMR and CIMS depend on spin accumulation effects. This is well known for CPP-GMR. For CIMS, this has been shown by experiments in which the spin accumulation profile is manipulated by introducing spin-flip scattering at different places in the structure<sup>5</sup>. It turns out that both the GMR effect and the spin transfer torque can be enhanced by introducing spin-flip scattering outside a F1/N/F2 trilayer (in the leads) or reduced by spin-flip scattering in the nonmagnetic layer N<sup>5</sup>. This calls for a unified theory of CPP-GMR and spin transfer torque, taking into account spin accumulation, spin relaxation, and both interface and bulk spin dependent scattering. This is actually the direction of most recent theoretical developments<sup>11,12,13</sup>.

The model we present in this paper fits directly with the interpretation of CPP-GMR data in the model of Valet and Fert (VF)<sup>14</sup>. Most of the parameters of our description can be derived directly from the analysis of CPP-GMR experimental data<sup>15</sup>, that is interface and

bulk spin asymmetry coefficients, interface resistance, layer resistivities, and spin diffusion lengths. As we will see below, two additional parameters, namely the real and imaginary parts of the mixing conductance<sup>13,16</sup>, are also needed. They can be derived from quantum-mechanical calculations<sup>17</sup> of the transmission of spin currents at the interface under consideration. By introducing into our model calculated values of the mixing conductance in addition to the set of parameters derived from GMR experiments, we calculate the current-induced torque for different types of structures in order to understand how its sign, amplitude and angular variation depend on the spin asymmetry coefficients and spin accumulation effects. The calculations of our model are based on macroscopic transport equations similar to those derived from the Boltzmann equation approach of the VF model<sup>14</sup> for the CPP-GMR of multilayers with collinear magnetizations. Stationary charge and spin current are described by classical diffusion equations. We assume that the absorption of the transverse component of the spin currents is quasi-interfacial, as this has been justified by a quantum description of the transmission of transverse spin current into a ferromagnetic layer. This assumption allows to derive some effective boundary conditions for the spin accumulation and spin current drops at the interfaces<sup>16</sup>, and this way also to calculate the torque acting on a magnetic film for an arbitrary angle between magnetic moments of the two ferromagnetic films in a structure. Thus, in a certain sense this extends to an arbitrary angle a small-angle description<sup>18</sup> that has been used for the interpretation of recent results<sup>6</sup>.

The paper is organized as follows. Macroscopic equations describing currents and spin accumulation inside the films are derived in section 2. The boundary conditions and general formulae for the torque in a four-layer structure are presented in sections 3 and 4, respectively. Numerical results for the structure with two magnetic films are presented and discussed in section 5. The limiting case of real mixing conductance is considered in section 6. The limit of a small angle between magnetizations is discussed in section 7, whereas final conclusions are in section 8.

## II. CURRENTS AND SPIN ACCUMULATION INSIDE MAGNETIC AND NONMAGNETIC FILMS

We assume the electrical current in the multilayer is carried by free-like electrons of equal concentrations in all the layers and without any spin polarization at equilibrium. The distribution function  $f$  inside the films is a  $2 \times 2$  matrix in the spin space, and its spatial variation can be described by the diffusion equation. We assume the distribution functions are uniform in the plane of the films, and vary only along the axis  $x$  normal to the films. Let us consider first ferromagnetic layers.

### A. Magnetic films

The diffusion equation for arbitrary spin quantization axis takes then the form<sup>16</sup>

$$\check{D} \frac{\partial^2 \check{f}}{\partial x^2} = \frac{1}{\tau_{sf}} \left[ \check{f} - \check{1} \frac{\text{Tr}\{\check{f}\}}{2} \right], \quad (1)$$

where  $\check{D}$  is the diffusion  $2 \times 2$  matrix in the spin space,  $\check{1}$  is the  $2 \times 2$  unit matrix, and  $\tau_{sf}$  is the spin-flip relaxation time. As it has been already mentioned in the introduction, we assume that the internal exchange field inside ferromagnetic metals is strong enough so that the component of the distribution function perpendicular to the local magnetization vanishes. Thus, the distribution function is diagonal when the spin quantization axis is parallel to the local spin polarization of the ferromagnetic system. Equation (1) can be then written as

$$D_{\uparrow} \frac{\partial^2 f_{\uparrow}}{\partial x^2} = \frac{1}{2\tau_{sf}} (f_{\uparrow} - f_{\downarrow}), \quad (2)$$

$$D_{\downarrow} \frac{\partial^2 f_{\downarrow}}{\partial x^2} = \frac{1}{2\tau_{sf}} (f_{\downarrow} - f_{\uparrow}), \quad (3)$$

where  $f_{\uparrow}$  and  $f_{\downarrow}$  are the distribution functions for spin-majority and spin-minority electrons, respectively.

The above system of two equations can be rewritten as

$$\frac{\partial^2 (f_{\uparrow} - f_{\downarrow})}{\partial x^2} = \frac{1}{l_{sf}^2} (f_{\uparrow} - f_{\downarrow}), \quad (4)$$

$$\frac{\partial^2 (f_{\uparrow} + f_{\downarrow})}{\partial x^2} = \eta \frac{\partial^2 (f_{\uparrow} - f_{\downarrow})}{\partial x^2}, \quad (5)$$

where

$$\frac{1}{l_{sf}^2} = \frac{1}{2} \left( \frac{1}{l_{\uparrow}^2} + \frac{1}{l_{\downarrow}^2} \right) \quad (6)$$

with  $l_{\uparrow}^2 = D_{\uparrow} \tau_{sf}$  and  $l_{\downarrow}^2 = D_{\downarrow} \tau_{sf}$ , and  $\eta$  defined as

$$\eta = - \frac{D_{\uparrow} - D_{\downarrow}}{D_{\uparrow} + D_{\downarrow}}. \quad (7)$$

Equations (4) and (5) can be rewritten in terms of the electro-chemical potentials  $\bar{\mu}_{\uparrow}$  ( $\bar{\mu}_{\downarrow}$ ) for spin-majority (spin-minority) electrons as

$$\frac{\partial^2 (\bar{\mu}_{\uparrow} - \bar{\mu}_{\downarrow})}{\partial x^2} = \frac{1}{l_{sf}^2} (\bar{\mu}_{\uparrow} - \bar{\mu}_{\downarrow}), \quad (8)$$

$$\frac{\partial^2 (\bar{\mu}_{\uparrow} + \bar{\mu}_{\downarrow})}{\partial x^2} = \eta \frac{\partial^2 (\bar{\mu}_{\uparrow} - \bar{\mu}_{\downarrow})}{\partial x^2}. \quad (9)$$

The above equations are equivalent to the equations derived from the Boltzmann equation approach by Valet and Fert<sup>14</sup>.

Solution of Eqs (8) and (9) gives

$$\begin{aligned} \bar{\mu}_\uparrow &= (1 + \eta)[A \exp(x/l_{sf}) \\ &+ B \exp(-x/l_{sf})] + Cx + G, \end{aligned} \quad (10)$$

and

$$\begin{aligned} \bar{\mu}_\downarrow &= (\eta - 1)[A \exp(x/l_{sf}) \\ &+ B \exp(-x/l_{sf})] + Cx + G, \end{aligned} \quad (11)$$

where  $A$ ,  $B$ ,  $C$  and  $G$  are constants to be determined later from the appropriate boundary conditions.

The electro-chemical potentials can be written as

$$\check{\mu} = \bar{\mu}_0 \check{1} + g \check{\sigma}_z \quad (12)$$

with

$$\bar{\mu}_0 = (\bar{\mu}_\uparrow + \bar{\mu}_\downarrow)/2 \quad (13)$$

and

$$g = (\bar{\mu}_\uparrow - \bar{\mu}_\downarrow)/2. \quad (14)$$

Thus, the explicit forms for  $\bar{\mu}_0$  and  $g$  are

$$\bar{\mu}_0 = \eta[A \exp(x/l_{sf}) + B \exp(-x/l_{sf})] + Cx + G, \quad (15)$$

and

$$g = A \exp(x/l_{sf}) + B \exp(-x/l_{sf}). \quad (16)$$

For an arbitrary quantization axis the particle and spin currents are given by the  $2 \times 2$  matrix  $\check{j}$  in the spin space

$$\check{j} = -\check{D} \frac{\partial \check{f}}{\partial x} = -\rho(E_F) \check{D} \frac{\partial \check{\mu}}{\partial x}, \quad (17)$$

where  $\rho(E_F)$  is the density of states at the Fermi level per spin (per unit volume and unit energy). When the quantization axis is parallel to the local spin polarization, one finds

$$\frac{1}{\rho(E_F)} j_\uparrow = -D_\uparrow C - \frac{\tilde{D}}{l_{sf}} [A \exp(x/l_{sf}) - B \exp(-x/l_{sf})], \quad (18)$$

$$\frac{1}{\rho(E_F)} j_\downarrow = -D_\downarrow C + \frac{\tilde{D}}{l_{sf}} [A \exp(x/l_{sf}) - B \exp(-x/l_{sf})], \quad (19)$$

where

$$\tilde{D} = 2 \frac{D_\uparrow D_\downarrow}{D_\uparrow + D_\downarrow}. \quad (20)$$

It is convenient to write the spin current in the matrix form as

$$\check{j} = \frac{1}{2} [j_0 \check{1} + j_z \check{\sigma}_z], \quad (21)$$

with  $j_0 = (j_\uparrow + j_\downarrow)$  being the total particle current density, and  $j_z = (j_\uparrow - j_\downarrow)$  being the total  $z$ -component of the spin current. Thus, one finds

$$\frac{1}{\rho(E_F)} j_0 = -C(D_\uparrow + D_\downarrow), \quad (22)$$

and

$$\frac{1}{\rho(E_F)} j_z = -C(D_\uparrow - D_\downarrow)$$

$$- \frac{2\tilde{D}}{l_{sf}} [A \exp(x/l_{sf}) - B \exp(-x/l_{sf})]. \quad (23)$$

The particle current  $j_0$  is related to the charge current  $I_0$  via  $I_0 = ej_0$ , where  $e$  is the electron charge ( $e < 0$ ). Thus, positive charge current (flowing from left to right) corresponds to negative particle current (electrons flow from right to left).

## B. Nonmagnetic films

Solution of the diffusion equation for the distribution functions inside nonmagnetic films leads to the following equation

$$\check{\mu} = \bar{\mu}_0 \check{1} + \mathbf{g} \cdot \check{\boldsymbol{\sigma}} \quad (24)$$

where  $\check{\boldsymbol{\sigma}} = (\check{\sigma}_x, \check{\sigma}_y, \check{\sigma}_z)$  and in a general case all the three components of  $\mathbf{g}$  are nonzero. The general solutions for  $\bar{\mu}_0$  and  $\mathbf{g}$  have the forms

$$\bar{\mu}_0 = Cx + G, \quad (25)$$

$$\mathbf{g} = \mathbf{A} \exp(x/l_{sf}) + \mathbf{B} \exp(-x/l_{sf}). \quad (26)$$

The spin currents are then given by

$$\check{j} = \frac{1}{2} (j_0 \check{1} + \mathbf{j} \cdot \check{\boldsymbol{\sigma}}), \quad (27)$$

with

$$\frac{1}{\rho(E_F)} j_0 = -2CD \quad (28)$$

and

$$\frac{1}{\rho(E_F)} \mathbf{j} = -\frac{2D}{l_{sf}} [\mathbf{A} \exp(x/l_{sf}) - \mathbf{B} \exp(-x/l_{sf})], \quad (29)$$

where now  $D_\uparrow = D_\downarrow \equiv D$ . Of course, all the constants may be different in different layers.

### C. Rotations of the quantization axis

Distribution function and spin current in the magnetic films are written in the coordinate system with the axis  $z$  along the local spin polarization. In turn, the formula given above for the distribution function and spin current inside nonmagnetic films have general form valid in arbitrary coordinate system. It is convenient, however, to write them in the system whose axis  $z$  coincides with the local quantization axis in one of the adjacent ferromagnetic films. Since the magnetic moments of the two ferromagnetic films are non-collinear, it will be necessary to transform the distribution function and spin current from one system to another. Thus, if the solution for electrochemical potentials in a given coordinate system has the form (24), then the solution in the coordinate system rotated by an angle  $\varphi$  about the axis  $x$  is still given by Eq.(24), but with  $\mathbf{g}$  replaced with  $\mathbf{g}'$  given by

$$g'_x = g_x, \quad (30)$$

$$g'_y = g_y \cos \varphi + g_z \sin \varphi, \quad (31)$$

$$g'_z = -g_y \sin \varphi + g_z \cos \varphi. \quad (32)$$

Similar relations also hold when transforming spin current  $\mathbf{j}$  from one coordinate system to the other one.

### III. BOUNDARY CONDITIONS AND TORQUE

To determine the unknown constants that enter the general expressions for electric current and distribution functions inside all the magnetic and nonmagnetic parts of any layered structure, we need to specify boundary conditions, which have to be fulfilled by the distribution function and currents at each interface. Such boundary conditions were derived by Brataas *et al*<sup>16</sup> within the phenomenological description, and here we will make use of them.

Charge and spin currents across the normal-metal-ferromagnet interface (called in the following interfacial currents), calculated on the normal-metal side in the coordinate system with the axis  $z$  along the local quantization axis in the ferromagnet, can be written as<sup>16</sup>:

$$e^2 j_0 = (G_\uparrow + G_\downarrow)(\bar{\mu}_0^F - \bar{\mu}_0^N) + (G_\uparrow - G_\downarrow)(g_z^F - g_z^N), \quad (33)$$

$$e^2 j_z = (G_\uparrow - G_\downarrow)(\bar{\mu}_0^F - \bar{\mu}_0^N) + (G_\uparrow + G_\downarrow)(g_z^F - g_z^N), \quad (34)$$

$$e^2 j_x = -2\text{Re}\{G_{\uparrow\downarrow}\}g_x^N + 2\text{Im}\{G_{\uparrow\downarrow}\}g_y^N, \quad (35)$$

$$e^2 j_y = -2\text{Re}\{G_{\uparrow\downarrow}\}g_y^N - 2\text{Im}\{G_{\uparrow\downarrow}\}g_x^N, \quad (36)$$

where  $\mathbf{g}^N$  ( $\mathbf{g}^F$ ) is the spin accumulation on the N (F) side of the N/F interface,  $G_\uparrow$  and  $G_\downarrow$  are the interfacial conductances in the spin-majority and spin-minority channels, and  $G_{\uparrow\downarrow}$  is the spin-mixing conductance of the interface, which comes into play only in non-collinear configurations. It is worth to point that the above boundary conditions are valid when there is no spin-flip scattering at the interface.

The boundary conditions can be specified as follows: (i) particle current is continuous across all interfaces (in all layers and across all interfaces it is constant and equal to  $j_0$ ), (ii) the spin current component parallel to the magnetization of a ferromagnetic layer is continuous across the interface between magnetic and nonmagnetic layers, and (iii) normal components (perpendicular to the magnetization of a ferromagnetic film) of the spin current vanish in the magnetic layer and there is a jump of these components at the interface between magnetic and nonmagnetic films, described by Eqs (35) and (36). The above boundary conditions have to be fulfilled at all interfaces. The number of the corresponding equations is then equal to the number of unknown constants, which allows one to determine the spin accumulation and the charge and spin currents.

Since the perpendicular component of the spin current is absorbed by the magnetic layers, the corresponding torque  $\boldsymbol{\tau}$  per unit square, exerted on a ferromagnetic film, can be calculated as

$$\boldsymbol{\tau} = \frac{\hbar}{2} (\mathbf{j}_{\perp L} - \mathbf{j}_{\perp R}), \quad (37)$$

where  $\mathbf{j}_{\perp L}$  and  $\mathbf{j}_{\perp R}$  are the normal (to the magnetization) components of the spin current at the left and right interfaces of the magnetic film, calculated on the normal metal side of these interfaces. In the simple case (as in Fig. 1), where there is no additional magnetic layer outside the F1/N/F2 trilayer and no transverse spin current at the outer edges of the trilayer,  $\boldsymbol{\tau}$  is simply given by  $\boldsymbol{\tau} = -\hbar\mathbf{j}_{\perp R}/2$  for F1 and  $\boldsymbol{\tau} = \hbar\mathbf{j}_{\perp L}/2$  for F2, where  $\mathbf{j}_{\perp R}$  and  $\mathbf{j}_{\perp L}$  have to be calculated in the nonmagnetic spacer layer (N) at the right interface of F1 and left interface of F2 (left and right interfaces of N), respectively.

### IV. TORQUE IN A SPIN-VALVE STRUCTURE

The structure F1/N/F2 under consideration consists of two left (thick) and right (thin) magnetic films, separated by a nonmagnetic layer. The thick magnetic film is assumed to be semi-infinite, so it also plays a role of the left lead. The thin magnetic film is followed by the right nonmagnetic lead, also assumed to be semi-infinite. Thickness of the nonmagnetic spacer layer is  $d_0$ , whereas of the thin magnetic film is  $d_2$ . Such a structure is shown schematically in Fig.1. Both ferromagnetic films are magnetized in their planes, and magnetization of the thin layer is rotated by an angle  $\varphi$  around the axis  $x$  (normal to the films) as shown in Fig.1. Axis  $z$  of the coordinate

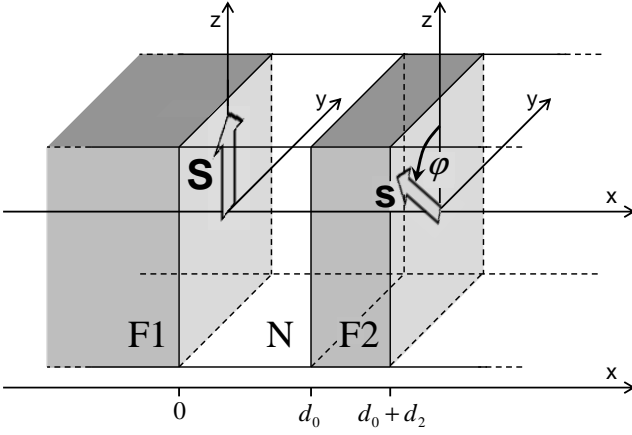


FIG. 1: Schematic structure of the system studied in this paper. The system consists of thick (F1) and thin (F2) ferromagnetic films, separated by a nonmagnetic (N) layer. The thick magnetic film (similarly as the right nonmagnetic lead) is assumed to be semi-infinite, while the thin nonmagnetic and ferromagnetic films have thicknesses  $d_0$  and  $d_2$ , respectively. The arrows indicate orientation of the net spin of the magnetic films, with  $\varphi$  being the angle between the spins.

system is along the net spin of the thick ferromagnetic film (opposite to the corresponding magnetization). In both ferromagnetic films the local quantization axes are along the local net spin, while as the global quantization axis we choose the local one in the thick ferromagnetic film. According to our definition, charge current  $I_0$  is positive when it flows along the axis  $x$  from left to right, i.e., from the thick towards thin magnetic films (electrons flow then from right to left).

The in-plane component  $\tau_{\parallel}$  of the torque acting on the thin magnetic film can be written as

$$\tau_{\parallel} = a \hat{\mathbf{s}} \times (\hat{\mathbf{s}} \times \hat{\mathbf{S}}), \quad (38)$$

where  $\hat{\mathbf{s}}$  and  $\hat{\mathbf{S}}$  are the unit vectors along the spin polarization of the thin and thick magnetic layers, respectively. The parameter  $a$  is a function of the charge current  $I_0$  (not indicated explicitly in Eq.(38)). Equation (38) can be rewritten in the form

$$\tau_{\varphi} = a \sin \varphi, \quad (39)$$

where the torque  $\tau_{\varphi}$  is defined in such a way that positive (negative) torque tends to increase (decrease) the angle  $\varphi$  ( $\varphi \in \langle 0, 2\pi \rangle$ ) between spin moments of the films.

The torque  $\tau_{\varphi}$  can be calculated from Eq.(37) as

$$\tau_{\varphi} = -\frac{\hbar}{2} j'_y|_{x=d_0} = -\frac{\hbar}{2} (j_z \sin \varphi + j_y \cos \varphi)|_{x=d_0}, \quad (40)$$

where  $j'_y$  and  $j_{z,y}$  are the components of spin current in the nonmagnetic thin film written in the local system of the thin and thick magnetic films, respectively, and calculated at the very interface between the nonmagnetic

an thin magnetic films. Comparison of Eqs (39) and (40) gives

$$a = -\frac{\hbar}{2 \sin \varphi} j'_y|_{x=d_0} = -\frac{\hbar}{2} (j_z + j_y \cot \varphi)|_{x=d_0}. \quad (41)$$

The out-of-plane (normal) component  $\tau_{\perp}$  of the torque may be generally written as

$$\tau_{\perp} = b \hat{\mathbf{s}} \times \hat{\mathbf{S}}, \quad (42)$$

where the parameter  $b$  depends on  $I_0$  (not indicated explicitly). It can be calculated from the formula

$$\tau_x = \frac{\hbar}{2} j'_x|_{x=d_0} = \frac{\hbar}{2} j_x|_{x=d_0}, \quad (43)$$

where  $j_x$  ( $j'_x$ ) is the  $x$ -component of the spin current in the nonmagnetic thin film taken at the interface between the two thin films and written in the coordinate system of the thick (thin) magnetic films ( $j_x = j'_x$  according to Eq.(30)). From Eqs (42) and (43) follows that the parameter  $b$  is equal

$$b = -\frac{\hbar}{2 \sin \varphi} j'_x|_{x=d_0} = -\frac{\hbar}{2 \sin \varphi} j_x|_{x=d_0}. \quad (44)$$

By taking into account Eqs (35) and (36) one can relate the torque directly to the spin accumulation in the nonmagnetic film taken at the interface with the thin magnetic layer. The in-plane (Eq.(40)) and out-of-plane (Eq.(43)) torque components can be then rewritten as

$$\begin{aligned} \tau_{\varphi} &= -\frac{\hbar}{e^2} [\text{Re}\{G_{\uparrow\downarrow}\} g'_y + \text{Im}\{G_{\uparrow\downarrow}\} g'_x]|_{x=d_0} \\ &= -\frac{\hbar}{e^2} [\text{Re}\{G_{\uparrow\downarrow}\} (g_y \cos \varphi + g_z \sin \varphi) \\ &\quad + \text{Im}\{G_{\uparrow\downarrow}\} g_x]|_{x=d_0}, \end{aligned} \quad (45)$$

and

$$\begin{aligned} \tau_x &= \frac{\hbar}{e^2} [\text{Re}\{G_{\uparrow\downarrow}\} g'_x - \text{Im}\{G_{\uparrow\downarrow}\} g'_y]|_{x=d_0} \\ &= \frac{\hbar}{e^2} [\text{Re}\{G_{\uparrow\downarrow}\} g_x - \text{Im}\{G_{\uparrow\downarrow}\} \\ &\quad \times (g_y \cos \varphi + g_z \sin \varphi)]|_{x=d_0}. \end{aligned} \quad (46)$$

Similarly, the constants  $a$  and  $b$  can be related to the spin accumulation *via* the formulae

$$\begin{aligned} a &= -\frac{\hbar}{e^2 \sin \varphi} [\text{Re}\{G_{\uparrow\downarrow}\} g'_y + \text{Im}\{G_{\uparrow\downarrow}\} g'_x]|_{x=d_0} \\ &= -\frac{\hbar}{e^2} \left[ \text{Re}\{G_{\uparrow\downarrow}\} (g_y \cot \varphi + g_z) + \text{Im}\{G_{\uparrow\downarrow}\} \frac{g_x}{\sin \varphi} \right]|_{x=d_0}, \end{aligned} \quad (47)$$

and

$$\begin{aligned} b &= \frac{\hbar}{e^2 \sin \varphi} [-\text{Re}\{G_{\uparrow\downarrow}\} g'_x + \text{Im}\{G_{\uparrow\downarrow}\} g'_y]|_{x=d_0} \\ &= \frac{\hbar}{e^2} \left[ -\text{Re}\{G_{\uparrow\downarrow}\} \frac{g_x}{\sin \varphi} + \text{Im}\{G_{\uparrow\downarrow}\} (g_y \cot \varphi + g_z) \right]|_{x=d_0}. \end{aligned} \quad (48)$$

Equations (40,43) and (41,44) are the final formula for the torque components and the parameters  $a$  and  $b$ , expressed in terms of the spin currents. Alternatively, Eqs (45) to (48) are the corresponding formula expressed in terms of the spin accumulation. For numerical calculations one can use either the former equations or equivalently the latter ones.

## V. NUMERICAL RESULTS

For numerical calculations it is convenient to define the bulk and interfacial spin asymmetry factors for ferromagnetic films according to the standard definitions<sup>14</sup>,

$$\rho_{\uparrow(\downarrow)} = 2\rho^*(1 \mp \beta) \quad (49)$$

and

$$R_{\uparrow(\downarrow)} = 2R^*(1 \mp \gamma), \quad (50)$$

where  $\rho_{\uparrow}$  and  $\rho_{\downarrow}$  are the bulk resistivities for spin-majority and spin-minority electrons, respectively;  $R_{\uparrow}$  and  $R_{\downarrow}$  are the interface resistances per unit square for spin-majority and spin-minority electrons, whereas  $\beta$  and  $\gamma$  are the bulk and interfacial spin asymmetry coefficients. The formula (49) will also be used for nonmagnetic films (with  $\beta = 0$ ). The conductances  $G_{\uparrow}$  and  $G_{\downarrow}$  (see Eqs (33,34)) are then  $G_{\uparrow} = 1/R_{\uparrow}$  and  $G_{\downarrow} = 1/R_{\downarrow}$ . The mixing conductance  $G_{\uparrow\downarrow}$  is generally a complex parameter with the imaginary part being usually one order of magnitude smaller than the real part.

The key bulk parameters which enter the description, i.e., mean free paths and diffusion constants can be expressed in a free electron model by the parameters defined in Eq. (49) and the relevant Fermi energy  $E_F$ . In numerical calculations we assume the same Fermi energy for both magnetic and nonmagnetic layers. The diffusion parameters  $D_{\uparrow(\downarrow)}$  are then calculated from the formulae (assuming free electron like model for conduction electrons),

$$D_{\uparrow(\downarrow)} = \frac{1}{3}v_F\lambda_{\uparrow(\downarrow)}, \quad (51)$$

where  $v_F = \sqrt{2E_F/m_e}$  is the Fermi velocity of electrons, and the mean free paths  $\lambda_{\uparrow(\downarrow)}$  are

$$\lambda_{\uparrow(\downarrow)} = \frac{m_e v_F}{ne^2 \rho_{\uparrow(\downarrow)}}, \quad (52)$$

with  $m_e$  denoting the electron mass and  $n = (1/6\pi^2)(2m_e E_F/\hbar^2)^{3/2}$  being the density of electrons per spin. Apart from this  $\rho(E_F)$  (see Eq.(17)) is given by  $\rho(E_F) = (1/4\pi^2)(2m_e/\hbar^2)^{3/2} E_F^{1/2}$ . For such a description (based on free electron like model) one finds  $\lambda_{\downarrow}/\lambda_{\uparrow} = (1 - \beta)/(1 + \beta)$ , and the parameter  $\eta$  defined by Eq.(7) is determined by  $\beta$  via the simple relation

$$\eta = -\beta. \quad (53)$$

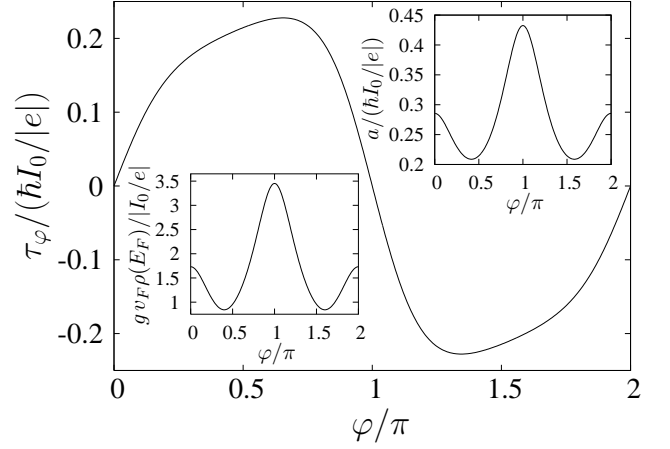


FIG. 2: Normalized in-plane torque  $\tau_{\varphi} = |\tau_{\parallel}|$  acting on the thin ferromagnetic film due to spin transfer, calculated as a function of the angle  $\varphi$  for parameters typical for Co/Cu system, as described in the text. The insets indicate the similarity between the angular dependence of the parameter  $a$  of the expression  $\tau_{\parallel} = a \hat{\mathbf{s}} \times (\hat{\mathbf{s}} \times \hat{\mathbf{S}})$  and that of the spin accumulation amplitude  $g$  (note that  $g$  is normalized to  $|I_0|$  whereas  $a$  to  $I_0$ ). The other parameters are:  $E_F = 7\text{eV}$ ,  $d_0 = 10\text{ nm}$ ,  $d_2 = 10\text{ nm}$ .

For nonmagnetic films we use the same definitions, but now  $\lambda_{\uparrow(\downarrow)}$  and  $D_{\uparrow(\downarrow)}$  are independent of the spin orientation (the corresponding  $\beta$  is equal to zero). Finally, the spin diffusion lengths will be assumed as independent parameters and will be taken from giant magnetoresistance experiments.

The parameters for the thick ferromagnetic film can be generally different from those for the thin magnetic film. Similarly, parameters corresponding to the two nonmagnetic components of the structure can also be different. In the following, however, we assume that the nonmagnetic spacer layer (N) and the right nonmagnetic lead are made of the same material.

The following four different situations have been recently studied experimentally<sup>6</sup>.

(i)  $\beta_1 = \beta_2 > 0$ ,  $\gamma_1 = \gamma_2 > 0$ , which corresponds to F1 and F2 of the same material with positive spin asymmetries for both bulk resistivities and interfacial resistances (this means spin-majority electrons are less scattered both inside the layers and at the interfaces).

(ii)  $\beta_1 > 0$ ,  $\gamma_1 > 0$ ,  $\beta_2 < 0$ ,  $\gamma_2 < 0$ , which corresponds to different materials for F1 and F2, with positive spin asymmetries for F1 and negative spin asymmetries for F2.

(iii)  $\beta_1 = \beta_2 < 0$ ,  $\gamma_1 = \gamma_2 < 0$ , which corresponds to the same material for F1 and F2, with negative spin asymmetries for both bulk resistivities and interfacial resistances.

(iv)  $\beta_1 < 0$ ,  $\gamma_1 < 0$ ,  $\beta_2 > 0$ ,  $\gamma_2 > 0$ , which corresponds to different materials for F1 and F2, with negative spin asymmetries for F1 and positive spin asymmetries for F2.

One of the systems within the category (i) is Co/Cu

structure, that has been extensively studied experimentally. For the bulk resistivities and the interface resistances we take the experimental values obtained from the GMR measurements<sup>15</sup>. Accordingly, for the Co layers we assume  $\rho_1^* = \rho_2^* = 5.1 \mu\Omega\text{cm}$ ,  $\beta_1 = \beta_2 = 0.51$ ,  $l_{sf}^{(1)} = l_{sf}^{(2)} = 60\text{nm}$ , whereas for the nonmagnetic Cu layers we assume  $\rho_0^* = 0.5 \mu\Omega\text{cm}$ ,  $l_{sf}^{(0)} = 10^3 \text{ nm}$ .

In turn, for the Co/Cu interfaces we assume  $R_1^* = R_2^* = 0.52 \cdot 10^{-15} \Omega\text{m}^2$  and  $\gamma_1 = \gamma_2 = 0.76$ . In principle, the corresponding mixing conductance  $G_{\uparrow\downarrow}$  could be derived from the angular dependence of the CPP-GMR. However, in practice there is a large uncertainty in this derivation and, according to the experimentalists who have performed this type of experiment<sup>19,20</sup>, there is no reliable experimental information on  $G_{\uparrow\downarrow}$  from GMR. Therefore, we assume the value calculated in a free-electron model corrected by certain factors taken from *ab-initio* calculations by Stiles<sup>21</sup>. For free electron gas and no reflection at the interface (we assumed the same Fermi energy in all layers), one finds the following relation between the spin current  $j'_y$  and the spin accumulation  $g'_y$  components (written in the coordinate system of the thin magnetic film and taken in the nonmagnetic spacer at the interface with the sensing (F2) magnetic film);  $j'_y = \rho(E_F)v_F g'_y/2 = 2G_{\uparrow\downarrow}^{\text{Sh}} g'_y/e^2$ . Here,  $G_{\uparrow\downarrow}^{\text{Sh}}$  is the Sharvin mixing conductance in the limit when there is no reflection at the interface,  $G_{\uparrow\downarrow}^{\text{Sh}} = e^2 k_F^2/4\pi h$ , with  $k_F$  the Fermi wavevector corresponding to the Fermi energy  $E_F$ . Reflection from the interface can be taken into account effectively *via* a phenomenological parameter  $Q$ , writing  $\text{Re}\{G_{\uparrow\downarrow}\} = QG_{\uparrow\downarrow}^{\text{Sh}}$ . In the case of Co/Cu system this factor is roughly equal to 0.925 according to Stiles<sup>21</sup>. Thus, in the following numerical calculations we assume  $\text{Re}\{G_{\uparrow\downarrow}\} = 0.542 \cdot 10^{-15} \Omega\text{m}^2$ . As for the imaginary part,  $\text{Im}\{G_{\uparrow\downarrow}\}$ , we determine it assuming the same ratio  $\text{Im}\{G_{\uparrow\downarrow}\}/\text{Re}\{G_{\uparrow\downarrow}\}$  as that following from *ab initio* calculations. Thus, we assume  $\text{Im}\{G_{\uparrow\downarrow}\} = 0.016 \cdot 10^{-15} \Omega\text{m}^2$ .

Numerical results on the in-plane and out-of-plane components of the torque as well as on the corresponding parameters  $a$  and  $b$  are shown in Fig.2 and Fig.3, respectively. The torque and the corresponding parameters  $a$  and  $b$  are normalized to  $\hbar I_0/|e|$ . Within the linear model assumed here the spin accumulation and spin currents are linear functions of the charge current, so the curves in Fig.2 are the same for arbitrary magnitude of the charge current  $I_0$ . Note that the sign of torque changes when  $I_0$  is reversed.

Figure 2 implies that a positive current ( $I_0 > 0$ ) tends to destabilize the parallel configuration and can switch it to antiparallel one above a certain threshold value. On the other hand a negative current tends to destabilize the antiparallel configuration. This behavior can be defined as a normal current-induced magnetic switching<sup>6</sup>. The numerical calculation of the switching currents is not the subject of our study here. We only note that, by using standard expressions of the switching currents as a function of the torque, magnetization, ap-

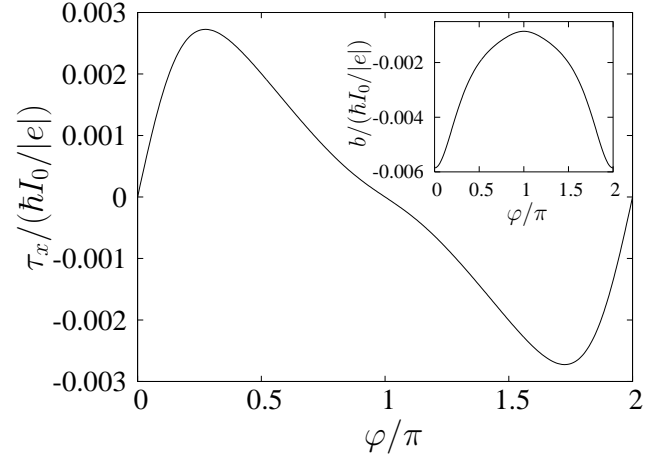


FIG. 3: Normalized out-of-plane torque, calculated as a function of the angle  $\varphi$  for the parameters typical for Co/Cu system. The inset shows the corresponding parameter  $b$ . The other parameters are the same as in Fig.2.

plied field, anisotropy field, Gilbert coefficient and thickness of the thin magnetic layer, one finds switching currents of the order of  $10^7 \text{ A/cm}^2$ . What we want to emphasize is the physical picture emerging from the plots of Fig.2. The main point is the similar angular dependence of the spin accumulation amplitude  $g = |g|$  in the nonmagnetic spacer and of the coefficient  $a$  in the expression (39) for the torque. This results from the relation between the transverse spin current and spin accumulation in the boundary conditions involving the mixing conductance, Eq.(36-37). The interpretation of the angular dependence is straightforward. The spin accumulation  $g$  is larger in the antiparallel configuration, when the spin direction predominantly transmitted by the thick layer is slowed down by the thin layer, i.e.  $g(\varphi = \pi) > g(\varphi = 0)$ . However,  $g(\varphi)$  does not increase monotonously from  $g(\varphi = 0)$  to  $g(\varphi = \pi)$ ; it begins with a decrease before getting at  $g(\varphi = \pi)$ . This initial decrease follows from the enhanced relaxation of the spin accumulation due to the efficient pumping of transverse spins as  $\varphi$  departs from zero. This transverse pumping decreases to zero when  $\varphi$  tends to  $\pi$  and  $g$  goes up to its maximum value  $g(\varphi = \pi)$ . The prefactor  $a = \tau_\varphi / \sin \varphi$  follows the same type of variation, with simply a slightly smaller initial decrease that can be explained by arguments related to the orientation of  $\mathbf{g}$ ,  $\hat{\mathbf{s}}$  and  $\hat{\mathbf{S}}$  (this will appear more clearly in section VI). Finally  $\tau_\varphi$  varies as  $a \sin \varphi$ , starting from zero as  $a(\varphi = 0)\varphi$  and going back to zero at  $\varphi = \pi$  as  $a(\varphi = \pi)(\pi - \varphi)$ , that is with a steeper slope if  $a(\varphi = \pi) > a(\varphi = 0)$ . The sort of a shoulder seen in Fig.2 for  $\varphi$  slightly below  $\pi/2$  is related to the minimum in  $g$  and  $a$  at about this angle.

The perpendicular component of the torque, that is the component coming from the imaginary part of  $G_{\uparrow\downarrow}$ , is shown in Fig.3, and is rather small, much smaller than the in-plane component (it would vanish for  $\text{Im}\{G_{\uparrow\downarrow}\} =$

0). Therefore, it plays a negligible role in the switching phenomenon, at least for Co/Cu(111). Although for other interfaces  $\text{Im}\{G_{\uparrow\downarrow}\}/\text{Re}\{G_{\uparrow\downarrow}\}$  is not as small as for Co/Cu(111), the imaginary part of the mixing conductance leads generally to perpendicular component of the torque which is definitely smaller than the in-plane one. Therefore, in the following we will deal only with the in-plane torque.

Let us consider now the remaining three cases described above; (ii), (iii) and (iv). For simplicity, we assume the same absolute values of the bulk and interface spin asymmetry coefficients  $\beta$  and  $\gamma$ , but their signs are adapted to each situation. The other parameters are the same for all the cases. The torque corresponding to the four situations is shown in Fig.4.

The solid curve in Fig.4(a) corresponds to the case (i), i.e.  $\beta_1 = \beta_2 > 0$ ,  $\gamma_1 = \gamma_2 > 0$ . This curve is the same as that shown in Fig.2, so that we will not discuss it here more. Let us change now the sign of the spin asymmetry parameters of the thin magnetic layer (case (ii) with  $\beta_2 < 0$ ,  $\gamma_2 < 0$ ). The corresponding torque, shown by the dashed line in Fig.4(a), has the same sign as in the case (i), so that the switching is still normal ( $I_0 > 0$  destabilizes the parallel state). With opposite spin asymmetry coefficients in F1 and F2, the spin accumulation  $g$  is larger in the parallel ( $\varphi = 0$ ) state than in the antiparallel ( $\varphi = \pi$ ) one, so that the torque now starts from zero at  $\varphi = 0$  with a slope that is steeper than the slope corresponding to the return point to zero at  $\varphi = \pi$ .

The solid line of Fig.4(b) corresponds to the case (iii) with negative values of all the spin asymmetry coefficients. Compared to Fig.4(a), the sign of the torque is now reversed, which means an inversion of the switching currents, as observed in FeCr/Cr/FeCr structures<sup>6</sup>. As the spin accumulation  $g$  in systems with similar materials for F1 and F2 is larger in the antiparallel configuration, the slope is higher at the point where the torque comes back to zero at  $\varphi = \pi$ .

Finally, for the dashed line of Fig.4(b) corresponding to the case (iv) ( $\beta_1 < 0$ ,  $\gamma_1 < 0$ ,  $\beta_2 > 0$ ,  $\gamma_2 > 0$ ), the switching is also inverse. This corresponds to the case studied in Ref.[6] with F1 (F2) and N corresponding to NiCr (permalloy) and Cu, respectively. Now, the spin accumulation is larger in the parallel state, so the torque approaches zero at  $\varphi = 0$  and  $\varphi = \pi$ , with the slope larger in the former case (at  $\varphi = 0$ ).

Basic characteristics of the switching phenomena in all the four cases are gathered in Table I, where the sign of the torque for positive current ( $I_0 > 0$ ) is given for  $\varphi$  in the range  $0 < \varphi < \pi$ . The normal/inverse switching phenomenon is correlated there with the sign of the corresponding GMR effect.

From the results described above follows that it is the spin asymmetry of the thick magnetic film, which determines whether the switching effect is normal or inverse. When this spin asymmetry is positive (negative), one finds a normal (inverse) switching phenomenon. It is also interesting to note that when the spin asymme-

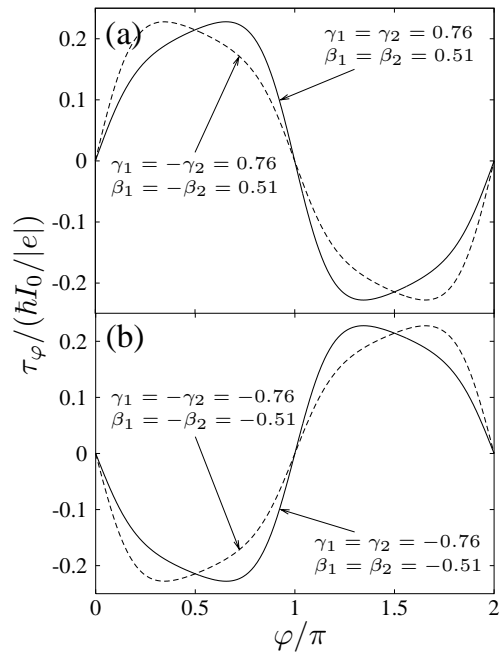


FIG. 4: Torque as a function of  $\varphi$  for the four situations described in the text, and for indicated values of the spin asymmetry parameters. The other parameters are the same as in Fig.2

tries of both magnetic films have the same sign, the structure shows normal GMR effect, whereas when they are opposite, the corresponding GMR effect is inverse as shown in many CPP-GMR measurements<sup>22</sup>. Experimental examples of the four behaviours of Table I can be found in the F1/N/F2 trilayers of Ref[6] respectively for NiFe/Cu/NiFe (i), NiFe/Cu/NiCr (ii), FeCr/Cr/FeCr (iii) and NiCr/Cu/NiFe (iv).

For the parameters used in numerical calculations described above the current-induced torque vanishes in collinear configurations and one of them (either parallel or antiparallel) is unstable. This leads to either normal or inverse switching phenomena. An interesting situation can occur when the amplitudes of spin asymmetry in the thick and thin layers are different. In Fig. 5, we show an example of torque calculated for  $\beta_1 = 0.1$  and  $\gamma_1 = -0.1$ ,  $\beta_2 = 0.51$  and  $\gamma_2 = 0.76$ . Let us first consider the case with  $I_0 > 0$ . The torque is positive when  $\varphi$  increases from zero, then comes back to zero at  $\varphi = \varphi_c$  and becomes negative between  $\varphi_c$  and  $\pi$ . This means that the torque tends to destabilize both the parallel and antiparallel states. Above some threshold value of the current for the instability of the parallel and antiparallel states, the only solution is a steady state precession (in the absence of anisotropy and demagnetizing field, there would be a stable equilibrium at an intermediate orientation between 0 and  $\pi$  in the layer plane, but the general solution is a precession).

In trilayers which have been studied up to now, steady precessions with generation of microwave oscillations



Situation	Spin asymmetries of magnetic layers		Sign of torque ( $0 < \varphi < \pi$ )		Sign of GMR
	Thick layer	Thin layer	Torque	Type	
(i)	$(\beta, \gamma) > 0$	$(\beta, \gamma) > 0$	$\tau > 0$	normal	GMR > 0 (normal)
(ii)	$(\beta, \gamma) > 0$	$(\beta, \gamma) < 0$	$\tau > 0$	normal	GMR < 0 (inverse)
(iii)	$(\beta, \gamma) < 0$	$(\beta, \gamma) < 0$	$\tau < 0$	inverse	GMR > 0 (normal)
(iv)	$(\beta, \gamma) < 0$	$(\beta, \gamma) > 0$	$\tau < 0$	inverse	GMR < 0 (inverse)

TABLE I: Characteristics of the current induced switching in the four cases studied in this paper. Correlation between the signs of the torque and GMR is also given.

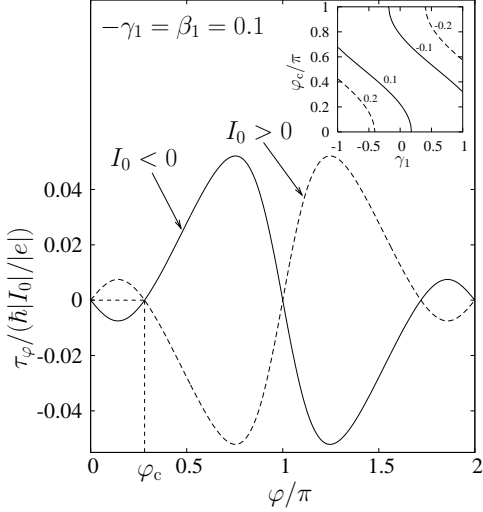


FIG. 5: Torque for the case when the spin asymmetry factors of the thick ferromagnetic film,  $\beta_1 = 0.1$  and  $\gamma_1 = -0.1$ , are significantly different from those of the thin one,  $\beta_2 = 0.51$  and  $\gamma_2 = 0.76$ . The torque is now normalized to  $|I_0|$  and the two curves correspond to  $I_0 > 0$  and  $I_0 < 0$ , as indicated. The angle  $\varphi_c$  corresponds to the point where the torque due to spin transfer vanishes. Inset shows variation of the angle  $\varphi_c$  with the spin asymmetry factor  $\gamma_1$  for several values of  $\beta_1$  indicated on the curves. The other parameters are as in Fig.2.

have been generally observed when a magnetic field is applied and in a given range of current density<sup>9</sup>. The possibility of obtaining microwave oscillations at zero field would be of great interest for several devices. Xiao et al<sup>23</sup> have predicted that microwave oscillations can be observed at zero field and in a given range of current density when, for asymmetric structures, the spin transfer and damping torques have markedly different angular dependences, so that their sum has a wavy angular dependence. In our structure of Fig.5, the existence of steady precessions at zero field has a different origin. It comes from the wavy angular dependence of the torque itself. This structure, with  $I_0 > 0$  would be of interest for the generation of oscillations at zero field and at any value of the current above some threshold value.

The behavior of Fig.5 for  $I_0 < 0$  has a different interest. Now, above some threshold value of the current, the spin transfer torque stabilizes both the parallel and antiparal-

lel states of the trilayer. In other words, it increases the damping of the system in both configurations. This is of interest for some devices, for example for stabilizing the configuration of read heads based on CPP-GMR against fluctuations or, at least, avoiding spin transfer induced fluctuations.

## VI. DISCUSSION IN THE LIMITING CASE OF REAL MIXING CONDUCTANCE

As it has been already mentioned before, the imaginary part of the mixing conductance is usually small. When  $\text{Im}\{G_{\uparrow\downarrow}\} = 0$ , the formulae (45) and (46) for the torque components acquire a simpler form. First of all, the out-of-plane components of the spin accumulation and spin current vanish,  $g_x = 0$  and  $j_x = 0$ . The in-plane torque can be then written in the form

$$\begin{aligned} \tau_\varphi &= -\frac{\hbar}{e^2} G_{\uparrow\downarrow} g'_y|_{x=d_0} \\ &= -\frac{\hbar}{e^2} G_{\uparrow\downarrow} (g_y \cos \varphi + g_z \sin \varphi)|_{x=d_0}, \end{aligned} \quad (54)$$

where  $G_{\uparrow\downarrow}$  is real. In turn, the out-of-plane torque vanishes then exactly,

$$\tau_x = 0. \quad (55)$$

When the spin accumulation in the layer N at its interface with the layer F2 forms an angle  $\varphi_g$  with the axis  $z$ , then one finds  $g'_y = g \sin(\varphi - \varphi_g)$  and the torque may be written in the form

$$\tau_\varphi = -\frac{\hbar}{e^2} G_{\uparrow\downarrow} g \sin(\varphi - \varphi_g), \quad (56)$$

where  $g$  is the absolute value (amplitude) of the spin accumulation at the interface. According to Eq.(41) the parameter  $a$  may be then expressed in the form

$$a = -\frac{\hbar}{e^2} G_{\uparrow\downarrow} g \frac{\sin(\varphi - \varphi_g)}{\sin \varphi}, \quad (57)$$

The formulae (56) and (57) relate the torque and the parameter  $a$  to the amplitude  $g$  of spin accumulation in the layer N at its interface with F2, and to the *sinus* of the angle  $(\varphi - \varphi_g)$  between the spin accumulation  $\mathbf{g}$  and the polarization axis of the thin ferromagnetic layer F2. It is interesting to look at the angular variation of these parameters. We have calculated

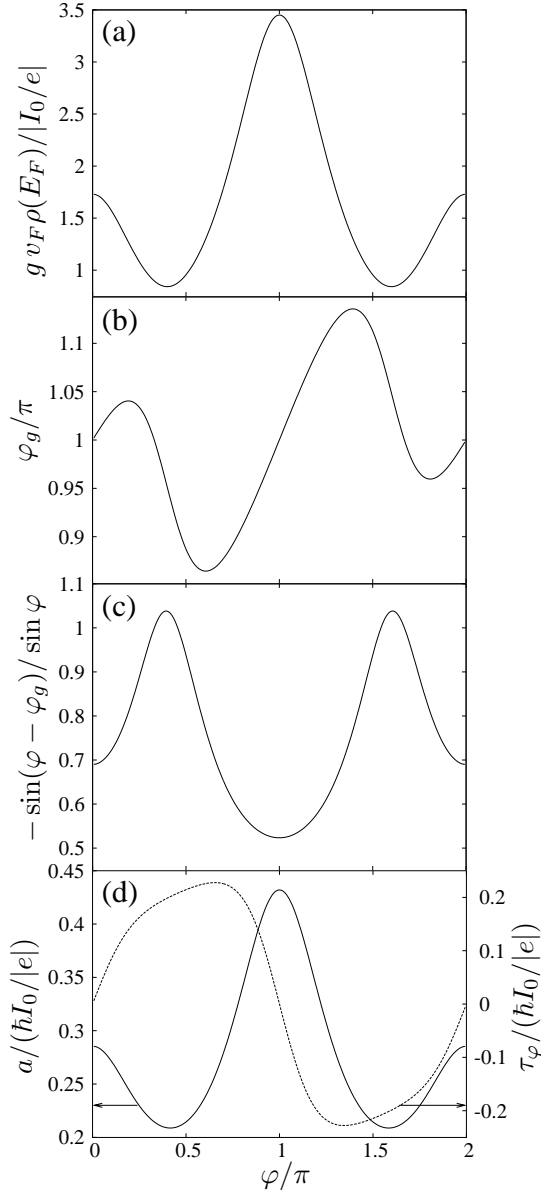


FIG. 6: Amplitude of spin accumulation at the interface (a), the angle  $\varphi_g$  (solid line in (b)), the factor  $\sin(\varphi - \varphi_g)/\sin \varphi$  (dashed line in (b)), the torque  $\tau_\varphi$  (dashed line in (c)), and the parameter  $a$  (solid line in (c)). All curves are calculated for  $\text{Im}G_{\uparrow\downarrow} = 0$  and for positive current,  $I_0 > 0$ . The other parameters are as in Fig.2.

them for the case (i) and in Fig.6 we show the angular variation of the spin accumulation amplitude  $g$ , the angle  $\varphi_g$ , the factor  $-\sin(\varphi - \varphi_g)/\sin \varphi$  of Eq.(57), the torque amplitude  $\tau_\varphi$ , and the prefactor  $a$  of the expression  $\tau_{\parallel} = a \hat{s} \times (\hat{s} \times \hat{S})$ . All the curves are shown there for positive current,  $I_0 > 0$ . The amplitude  $g$  of the spin accumulation, see Fig.6(a), goes from its small value in the parallel state to its higher value in the antiparallel state, as expected when F1 and F2 have the same spin asymmetries. As discussed in section V, the initial decrease

before the upturn to  $g$  in the antiparallel state is due to the relaxation enhancement generated by transverse spin pumping in a non-collinear state. As for the orientation of  $\mathbf{g}$ , one can see from the variation of  $\varphi_g$  in Fig.6(b) that the vector  $-\mathbf{g}$  has first an intermediate orientation between those of  $\hat{S}$  and  $\hat{s}$ , following the rotation of  $\hat{s}$  at an angle of about  $0.7\varphi$  from  $\hat{s}$ . Then  $-\mathbf{g}$  comes back to the orientation of  $\hat{S}$  and, as  $\varphi$  tends to  $\pi$ , the angle between  $-\mathbf{g}$  and  $\hat{S}$  tends to 0 as  $-0.55(\pi - \varphi)$ . The result of this angular variation of the spin accumulation is that the factor  $-\sin(\varphi - \varphi_g)/\sin \varphi$  does not change significantly and varies only between about 0.52 and 1.05 for the system we have considered, as shown in Fig.6(c). This indicates that the variation of the torque prefactor  $a$ , shown in Fig.6(d), is mainly controlled by the variation of the spin accumulation amplitude  $g$ , with a small additional influence of the factor  $-\sin(\varphi - \varphi_g)/\sin \varphi$  (this influence explains, for example, that the dip around  $\varphi = 0.45\pi$  is less pronounced for  $a$  than for  $g$ ). Finally the variation of  $\tau_\varphi$  with the angle  $\varphi$ , dashed curve in Fig.6(d), reflects the variation of the product of  $a$  times  $\sin \varphi$ .

We have seen in section V that similar angular variation of  $g$  and  $a = \tau_\varphi/\sin \varphi$  also occurs in the general case with nonzero but small imaginary part of  $G_{\uparrow\downarrow}$ . The explanation is the same as above, but only a little more complex because  $\mathbf{g}$  has also a normal component. The general conclusion is that the torque is closely related to the spin accumulation in the nonmagnetic layer N. We put forward two practical consequences of this correlation. (1) The ratio between the switching current amplitudes of the parallel $\rightarrow$ antiparallel and antiparallel $\rightarrow$ parallel transitions, which reflects approximately the ratio between the derivatives  $d\tau_\varphi/d\varphi$  at  $\varphi = 0$  and  $\varphi = \pi$ , simply reflects the ratio between  $g$  in the parallel and antiparallel configurations. In particular this ratio is inverted when the sign of the spin asymmetries is inverted in one of the magnetic layers, as in the situations (iii) and (iv) in section V. (2) More generally, the torque amplitude can be enhanced or reduced by enhancing or reducing the spin accumulation in the nonmagnetic spacer. This has been confirmed by the experiments of Ref.[6] in which the torque could be enhanced or reduced by introducing spin-flip scatterers at different places in the structure.

## VII. COMPARISON WITH THE PREVIOUS CALCULATION OF THE TORQUE FOR $\varphi$ CLOSE TO 0 OR $\pi$

A simple expression of the current-induced torque has been derived by Fert et al<sup>18</sup> in the small angle limit, that is when the angle  $\varphi$  between the two magnetic layers ( $\theta$  in the notation of Ref.[18]) is small or close to  $\pi$ . This expression involves also parameters derived from CPP-GMR data and has been recently fitted with experimental results of CIMS on samples doped in several ways<sup>6</sup>. It is interesting to compare the torques at small angle cal-

culated with this expression and by using the model of the present article. For simplicity, we will compare the two calculations when the mixing conductance is real, which allows us a clearer physical picture of the differences between the two approaches. With zero imaginary mixing conductance ( $\epsilon = 0$  in the notation of Ref.[18]), the expression of the torque at small angle is given by Eq.(5) of Ref.[18],

$$\tau = \hbar \left[ \left( \frac{v_F m_N^{\text{P(AP)}}}{8} + \frac{j_{m,N}^{\text{P(AP)}}}{2} \right) (1 - e^{-d_0/\lambda}) + \left( \frac{v_F m_{F1}^{\text{P(AP)}}}{4} + j_{m,F1}^{\text{P(AP)}} \right) e^{-d_0/\lambda} \right] \hat{\mathbf{s}} \times (\hat{\mathbf{s}} \times \hat{\mathbf{S}}), \quad (58)$$

where  $m_N^{\text{P(AP)}}(j_{m,N}^{\text{P(AP)}})$  is the spin accumulation density (spin current) in the N layer at the N/F2 interface in the parallel (P) and antiparallel (AP) configurations,  $m_{F1}^{\text{P(AP)}}(j_{m,F1}^{\text{P(AP)}})$  are the same quantities in F1 at the F1/N interface ( $m$  and  $j_m$  are defined as positive for polarizations in the majority spin direction of F1, note also that, in the notation of Ref.[18], one electron counts for 1/2 in  $m$  and  $j_m$ ) and  $\lambda$  is the mean free path in N. The torque we have calculated in the preceding sections corresponds to the first and dominant term of this expression in the limit  $d_0 \gg \lambda$  (we will come back later to the meaning of the other terms). Omitting the last three terms, Eq.(58) can be written as

$$\tau = \hbar \frac{v_F m_N^{\text{P(AP)}}}{8} \hat{\mathbf{s}} \times (\hat{\mathbf{s}} \times \hat{\mathbf{S}}). \quad (59)$$

The spin accumulation density  $m$  can be written as a function of the spin accumulation  $g$  of our paper in the following way:

$$m = \frac{m_e k_F}{2\pi^2 \hbar^2} g \quad (60)$$

so that Eq.(59) can be written as

$$\tau = \frac{\hbar}{2e^2} G_{\uparrow\downarrow}^{Sh} g \hat{\mathbf{s}} \times (\hat{\mathbf{s}} \times \hat{\mathbf{S}}), \quad (61)$$

to be compared with the torque found in section VI:

$$\tau = -\frac{\hbar}{e^2} G_{\uparrow\downarrow} g \frac{\sin(\varphi - \varphi_g)}{\sin \varphi} \hat{\mathbf{s}} \times (\hat{\mathbf{s}} \times \hat{\mathbf{S}}). \quad (62)$$

The only differences between Eqs.(61) and (62) are:

(i) The replacement of  $G_{\uparrow\downarrow}^{Sh}$  by  $G_{\uparrow\downarrow}$ . In section V, we assumed  $G_{\uparrow\downarrow}$  equal to  $0.925 \times G_{\uparrow\downarrow}^{Sh}$  for Co/Cu interface. The factor 0.925 is also the factor  $t$  which was approximated by 1 between Eq.(4) and Eq.(5) in Ref.[18]).

(ii) The replacement of the factor 1/2 by the value of  $-\sin(\varphi - \varphi_g)/\sin(\varphi)$  for  $\varphi$  close to 0 and  $\pi$  - approximately by 0.7 and 0.52 in the case illustrated in Fig.6(b).

Actually the factor 1/2 in Eq.(61) comes from the values  $\varphi_g = \pi + \varphi/2$  for  $\varphi$  infinitesimally small ( $\theta_m = \theta/2$  in the notation of Ref.[18]) and  $\varphi_g = \pi - (\pi - \varphi)/2$  for  $\pi - \varphi$  infinitesimally small. These values of  $\varphi_g$  are derived from a transverse spin conservation condition with the assumption of a constant orientation of  $\mathbf{g}$  in a thin enough nonmagnetic layer. Our calculations in this paper show that, for a Cu layer of 10 nm, this assumption does not strictly hold and that the factor 0.5 must be replaced by 0.7 and 0.52 for  $\varphi$  close respectively to 0 and  $\pi$ .

We thus conclude that the torques expressed respectively by Eq.(61), that is derived from the first term in the expression of the torque in Ref.[18], and by Eq.(62) derived in this article, differ only by a numerical factor not very different from unity. This factor will tend to unity for thinner N and will depart more from unity for thicker layer N.

It remains to discuss why our calculations do not include the three last terms of Eq.(58). This comes from the mixing conductance approximation<sup>13</sup>, that is the approximation of the boundary equations for the transverse components, Eqs.(35,36). These equations express the diffusion transverse spin current generated by the discontinuity between the finite value of  $\mathbf{g}_\perp$  ( $\mathbf{g}_\perp$  denotes the spin accumulation component normal to the magnetization) in N and its zero value in F. The finite value of  $\mathbf{g}_\perp$  is taken just at the interface, which assumes that the gradient of  $\mathbf{g}_\perp$  and the resulting variation of  $\mathbf{g}_\perp$  on a distance of the order of the mean free path can be neglected. The second term of Eq.(58) takes into account the contribution from this gradient to the diffusion current. In addition, if N is thinner than the mean free path, a certain amount of the diffusion current comes directly from F1, which gives rise to the last two terms of Eq.(58). In conclusion, the calculation of the torque at small angle in this article has the advantage of a more accurate determination of the orientation of the spin accumulation in the nonmagnetic spacer, that is, for example, a more accurate determination of the factor  $\sin(\varphi - \varphi_g)/\sin \varphi$  involved in Eq.(62). In the system we considered, the difference is relatively small (for a 10 nm thick spacer, 5% and 40% for  $\varphi$  close respectively to 0 and  $\pi$ ), and it should decrease (increase) for thinner (thicker layers). On the other hand, with the boundary conditions of Eqs.(35,36), we are not able to calculate the contributions to the diffusion current due to the gradient of spin accumulation and to the direct diffusion from the thick magnetic layers. These contributions, corresponding to the last three terms of Eq.(58), must be taken into account for thin nonmagnetic spacers – the diffusion from the thick layer vanishes only when the spacer is thicker than the mean free path. We will introduce them in a further extension of our model.

## VIII. CONCLUDING REMARKS

In conclusion, we have presented a model of CIMS which is partly based on the classical transport equations derived from the Boltzmann equation standard model of CPP-GMR<sup>14</sup>. Additional boundary equations based on the concept of mixing conductance are used to describe the interfacial absorption of transverse spin currents in non-collinear magnetic configurations. This model applied to Co/Cu/Co trilayers allows us to calculate the spin transfer torques as a function of the usual parameters derived from CPP-GMR measurements (interface spin asymmetry coefficients and resistances, bulk spin asymmetry coefficients and resistivities, spin diffusion lengths), and the mixing conductance coefficients derived from ab initio calculations. We have also shown that the torque and its angular dependence is closely related to the spin accumulation in the nonmagnetic spacer and to its angular dependence. Enhancing the spin accumulations seems to be the way to reduce the critical currents. The model has been also applied to situations with different spin asymmetries in the two magnetic lay-

ers of F1/N/F2 structures to reproduce the inversion of the switching current recently obtained by reversing the spin asymmetry of the thick magnetic layer. By applying it to asymmetric structures, we have shown that steady precessions can be obtained in zero field. We have also pointed out some application limits for boundary conditions and indicated that certain corrections can be anticipated by going beyond these limits.

## Acknowledgments

This work is partly supported by Polish State Committee for Scientific Research through the Grants No. PBZ/KBN/044/P03/2001, No. 2 P03B 053 25, and by the "Spintronics" RT Network of the EC RTN2-2001-00440 and FCT Grant No. POCTI/FIS/58746/2004. One of us (AF) thanks Vincent Cros, Julie Grollier and Henri Jaffres for very fruitful discussions. We also thank Mark Stiles for having communicated to us numerical data concerning the transmission of transverse spin currents at the Co/Cu(111) interface.

- 
- <sup>1</sup> J. C. Slonczewski, J. Magn. Magn. Mater. **159**, L1 (1996); **195**, L261 (1999).
  - <sup>2</sup> L. Berger, Phys. Rev. B **54**, 9353 (1996).
  - <sup>3</sup> M. Tsoi, A.G.M. Jansen, J. Bass, W.-C. Chiang, M. Seck, V. Tsoi, and P. Wyder, Nature (London) **406**, 46 (1998); E.B. Myers, D.C. Ralph, J.A. Katine, R.N. Louie, and R.A. Buhrman, Science **285**, 867 (1999); J.E. Wegrowe, D. Kelly, T. Truong, Ph. Guittienne, and J.Ph. Ansermet, Europhys. Lett **56**, 748 (2001).
  - <sup>4</sup> J. A. Katine, F.J. Albert, R.A. Buhrman, E.B. Myers, and D.C. Ralph, Phys. Rev. Lett. **84**, 3149 (2000); J. Grollier, V. Cros, A. Hamzic, J.M. George, H. Jaffres, A. Fert, G. Faini, J. Ben Youssef, and H. Legall, Appl. Phys. Lett. **78**, 3663 (2001); J.Z. Sun, D.J. Monsma, D.W. Abraham, M.J. Rooks, and R.H. Koch, Appl. Phys. Lett. **81**, 2202 (2002).
  - <sup>5</sup> S. Urazhdin, N. O. Birge, W. P. Pratt, and J. Bass, Appl. Phys. Lett. **84**, 1516, (2004).
  - <sup>6</sup> M.AlHajDarwish, H. Kurt, S. Urazhdin, A. Fert, R. Loloee, W.P. Pratt Jr., and J. Bass, Phys. Rev. Lett., **93**, 157203 (2004).
  - <sup>7</sup> M.N. Baibich, J.M. Broto, A. Fert, F. Nguyen van Dau, F. Petroff, P. Etienne, G. Creuzet, A. Friederich and J. Chazelas, Phys. Rev. Letters **61**, 2472 (1988); G. Binasch, P. Grünberg, F. Saurenbach, and W. Zinn, Phys. Rev. B **39**, 4828 (1989); J. Barnaś, A. Fuss, R.E. Camley, P. Grünberg and W. Zinn, Phys. Rev. B **42**, 8110 (1990).
  - <sup>8</sup> J. S. Moodera, L. R. Kinder, T. M. Wong and R. Meservey, Phys. Rev. Lett. **74**, 3273 (1995).
  - <sup>9</sup> S. I. Kiselev, J. C. Sankey, I. N. Krivorotov, N. C. Emley, R. J. Schoelkopf, R. A. Buhrman and D. C. Ralph, Nature **425**, 380 (2003); S. I. Kiselev, J. C. Sankey, I. N. Krivorotov, N. C. Emley, M. Rinkoski, C. Perez, R. A. Buhrman, and D. C. Ralph, Phys. Rev. Lett. **93**, 036601 (2004) ; W. H. Rippard, M. R. Pufall, S. Kaka, S. E. Russek, and T. J. Silva, Phys. Rev. Lett. **92**, 027201 (2004); W. H. Rippard, M. R. Pufall, S. Kaka, T. J. Silva, and S. E. Russek, Phys. Rev. B **70**, 100406(R) (2004).
  - <sup>10</sup> X. Waintal E.B. Myers, P.W. Brouwer, and D.C. Ralph, Phys. Rev. B **62**, 12317 (2000); Yu.A. Bazaliy, B.A. Jones, and S.C. Zhang, Phys. Rev. B **57**, R3213 (1998); J.E. Wegrowe, Phys. Rev. B **62**, 1 (2000); P. Weinberger, A. Vernes, B.L. Gyrfy and L. Szunyogh, Phys. Rev. B **70**, 094401 (2004); D.M. Edwards, F. Frederici, J. Mathon and A. Umerski, cond-mat/0407562.
  - <sup>11</sup> J. Slonczewski, J. Magn. Magn. Mat.. **247**, 324 (2002); L. Berger, J. Appl. Phys. **89**, 5521 (2001); S. Zhang, P. M. Levy, and A. Fert, Phys. Rev. Lett. **88**, 236601 (2002); A. Shpiro, P. M. Levy, and S. Zhang, Phys. Rev. B **67**, 104430 (2003).
  - <sup>12</sup> M.D. Stiles and A. Zangwill, Phys. Rev. B **66**, 014407 (2002); J. Appl. Phys. **91**, 6812 (2002).
  - <sup>13</sup> A. Brataas, Yu.V. Nazarov, and G.E.W. Bauer, Phys. Rev. Lett. **84**, 2481 (2000); D.H. Hernandez, Yu.V. Nazarov, A. Brataas, and G.E.W. Bauer, Phys. Rev. B **62**, 5700 (2000); Y. Tserkovnyak and A. Brataas Phys. Rev. B **65**, 094517 (2002); Y. Tserkovnyak, A. Brataas, and G.E.W. Bauer, Phys. Rev. Lett., **88**, 117601 (2002); Y. Tserkovnyak, A. Brataas, G.E.W. Bauer, and B.I. Halperin, cond-mat/0409242; A. A. Kovalev, A. Brataas, and G. E. W. Bauer, Phys. Rev. B **66**, 224424 (2002).
  - <sup>14</sup> T. Valet, A. Fert, Phys. Rev. B, **48**, 7099 (1993).
  - <sup>15</sup> J. Bass and W. P. Pratt Jr., J. Magn. Magn. Mat. **200**, 274 (1999).
  - <sup>16</sup> A. Brataas, Yu. V. Nazarov, G. E. W. Bauer, Eur. Phys. J. B **22**, 99, (2001).
  - <sup>17</sup> K. Xia, P. J. Kelly, G. E. W. Bauer, A. Brataas, and I. Turek, Phys. Rev. B, **65**, 220401 (2002); M. Zwierzycki, Y. Tserkovnyak, P. J. Kelly, A. Brataas, and G. E. W. Bauer, arXiv:cond-mat/0402
  - <sup>18</sup> A. Fert, V. Cros, J.M. George, J. Grollier, H. Jaffrès, A.

- Hamzic, A. Vaurès, G. Faini, J. Ben Youssef, and H. Le Gall, J. Magn. Magn. Metals (2004).
- <sup>19</sup> W.P. Pratt, private communication
- <sup>20</sup> P. Dauguet, P. Gandit, J. Chaussy, S.F. Lee, A. Fert, P. Holody, Phys. Rev. B54, 1083 (1996).
- <sup>21</sup> M.D. Stiles, private communication.
- <sup>22</sup> C. Vouille, A. Barthèlèmy, A. Fert, P.A. Schroeder, S. Hsu, A. Reilly, R. Loloee, Phys. Rev. B 60, 6710 (1999).
- <sup>23</sup> J. Xiao, A. Zangwill, and M.D. Stiles, Phys. Rev. B 70, 172405 (2004).